

Published in final edited form as:

Bioconjug Chem. 2011 December 21; 22(12): 2415–2422. doi:10.1021/bc200197h.

Comparison Study of [¹⁸F]FAI-NOTA-PRGD2, [¹⁸F]FPPRGD2 and [⁶⁸Ga]Ga-NOTA-PRGD2 for PET Imaging of U87MG Tumors in Mice

Lixin Lang^{1,ξ}, Weihua Li^{1,2,ξ}, Ning Guo¹, Ying Ma¹, Lei Zhu¹, Dale O. Kiesewetter¹, Baozhong Shen², Gang Niu^{1,3}, and Xiaoyuan Chen^{1,*}

¹Laboratory of Molecular Imaging and Nanomedicine (LOMIN), National Institute of Biomedical Imaging and Bioengineering (NIBIB), National Institutes of Health (NIH), Bethesda, MD 20892

²Department of Medical Imaging and Nuclear Medicine, the Fourth Affiliated Hospital, Harbin Medical University, Harbin 150001, China

³Imaging Sciences Training Program, Radiology and Imaging Sciences, Clinical Center and National Institute Biomedical Imaging and Bioengineering, NIH, Bethesda, Maryland, 20892, USA

Abstract

[¹⁸F]FPPRGD2, an F-18 labeled dimeric cyclic RGDyK peptide, has favorable properties for PET imaging of angiogenesis by targeting the $\alpha_v\beta_3$ integrin receptor. This radiotracer has been approved by the FDA for use in clinical trials. However, the time-consuming multiple-step synthetic procedure required for its preparation may hinder the widespread usage of this tracer. The recent development of a method using an F-18 fluoride-aluminum complex to radiolabel peptides provides a strategy for simplifying the labeling procedure. On the other hand, the easy-to-prepare [⁶⁸Ga]-labeled NOTA-RGD derivatives have also been reported to have promising properties for imaging $\alpha_v\beta_3$ integrin receptors. The purpose of this study was to prepare [¹⁸F]FPPRGD2, [¹⁸F]FAI-NOTA-PRGD2, and [⁶⁸Ga]Ga-NOTA-PRGD2 and to compare their pharmacokinetics and tumor imaging properties using small animal PET. All three compounds showed rapid and high tracer uptake in U87MG tumors with high target-to-background ratios. The uptake in the liver, kidneys and muscle were similar for all three tracers and they all showed predominant renal clearance. In conclusion, [¹⁸F]FAI-NOTA-PRGD2 and [⁶⁸Ga]Ga-NOTA-PRGD2 have imaging properties and pharmacokinetics comparable to those of [¹⁸F]FPPRGD2. Considering their ease of preparation and good imaging qualities, [¹⁸F]FAI-NOTA-PRGD2 and [⁶⁸Ga]Ga-NOTA-PRGD2 are promising alternatives to [¹⁸F]FPPRGD2 for PET imaging of tumor $\alpha_v\beta_3$ integrin expression.

Keywords

positron emission tomography (PET); integrin $\alpha_v\beta_3$; Arg-Gly-Asp (RGD) peptide; fluorine-aluminum complex; Ga-68; F-18

*Correspondence should be addressed to: Xiaoyuan Chen, Ph.D., Laboratory of Molecular Imaging and Nanomedicine (LOMIN), National Institute of Biomedical Imaging and Bioengineering (NIBIB), National Institutes of Health (NIH), Bethesda, MD 20892, USA, Bldg. 31, Room 1C22, Tel: 301-451-4246, Fax: 301-480-0679, shawn.chen@nih.gov.

^ξThese two authors contributed equally.

Introduction

Tumor angiogenesis is the process of new blood vessel formation necessary for tumor growth and metastasis,¹ and the integrin $\alpha_v\beta_3$ receptor plays an important role in promoting, sustaining and regulating the angiogenesis.^{2,3} In recent years, major efforts and progress have been made in the development of radiolabeled Arg-Gly-Asp (RGD) containing peptides to image tumor angiogenesis by targeting integrin $\alpha_v\beta_3$ receptors in various types of tumors.^{4,5} It is widely accepted that imaging tumor angiogenesis can be used not only for early detection of cancers, but also for monitoring treatment outcomes.^{4,6-9} Cyclic RGD peptides with various modifications have been labeled with ^{99m}Tc ¹⁰ and ^{111}In ¹¹ for SPECT imaging and labeled with ^{18}F ¹², ^{64}Cu ¹³, ^{68}Ga ^{14,15} and ^{89}Zr ¹⁶ for PET imaging. The peptide modifications have included dimerization and polymerization of up to 8 cyclic RGD peptide units to increase binding affinity, and the attachment of polar functional groups--such as sugar and polyethylene glycol (PEG)--to increase renal excretion.^{17,18} [^{18}F]FPPRGD2, an F-18 labeled dimeric cyclic RGDyK peptide with mini-PEGylation, has favorable properties for PET imaging of tumor angiogenesis, and it has been approved by the FDA for use in clinical trials.^{18,19}

F-18 is the most widely used positron emitting radioisotope for PET imaging, and its physical properties are ideally suited for RGD peptide-based PET imaging probes. The majority of methods used in labeling RGD peptides with ^{18}F use a prosthetic group, such as *N*-succinimidyl 4- [^{18}F]fluorobenzoate ([^{18}F]SFB)²⁰ or 4-nitrophenyl 2- [^{18}F]fluoropropionate ([^{18}F]NFPF),⁷ and the time-consuming multiple-step synthetic procedure required for preparation may hinder the widespread use of these ^{18}F -labeled RGD tracers. The preparation of [^{18}F]FPPRGD2 also faces these challenges. Efforts have been made with some success to simplify the labeling procedure by direct labeling of RGD peptides with a pre-attached functional group with a proper leaving group for fluoride displacement.²¹ On the other hand, labeling radioactive metal ions through a pre-attached chelator on RGD peptides has been blessed with a much simpler procedure. One advantage of using coordination chemistry is that only very small amounts of chelators are required to reach high labeling yield, which allows the radiotracer to be prepared without the need of HPLC purification, while maintaining reasonable specific activity levels. The easy preparations of ^{68}Ga -labeled NOTA-RGD derivatives are examples that have been reported to have promising properties for tumor imaging.^{14,15,22}

Application of chelation chemistry has led to recent discovery and development of ^{18}F fluoride-aluminum complexes to radiolabel peptides that provide a strategy to simplify the labeling procedure.^{23,24} The goal of this study was to prepare [^{18}F]FPPRDG2, [^{18}F]FAI-NOTA-PRGD2, and [^{68}Ga]Ga-NOTA-PRGD2 from the same pegylated dimeric RGD peptide PEG3-E[c(RGDyK)]₂ (denoted as PRGD2) and to compare their pharmacokinetics and imaging properties in a U87MG glioblastoma xenograft model using microPET.

Materials and methods

The p-SCN-Bn-NOTA was purchased from Macrocyclics (Dallas, TX) and PRGD2 was obtained from Peptides International (Louisville, KY). All of the other chemicals were purchased from Sigma-Aldrich. A Waters 600 high-performance liquid chromatography (HPLC) system with a Waters 996 Photodiode Array Detector (PDA) using a preparative C₁₈ HPLC column (PROTO 300 C₁₈ 5 μm , 250 \times 20 mm, Higgins Analytical, Inc.) was used for peptide purification. A Varian BOND ELUT C₁₈ column (100 mg) was used for solid phase extraction. Another Waters 600 HPLC pump with a Waters 996 PDA and an online radioactivity detector (Beckman) using a semi-prep C₁₈ HPLC column (Vydac C₁₈ peptide & protein 5 μm , 250 \times 10 mm, Grace Davison) was used for purification of

radiolabeled compounds. A Perkin-Elmer 200 series HPLC pump with a Waters 2487 UV detector and a Bioscan Flow-Count detector using an analytical C₁₈ HPLC column (Vydac C₁₈ peptide & protein 5 μm, 250 × 4.6 mm, Grace Davison) was used for analysis or purification of labeled compounds. Mass spectra were obtained with a Waters LC-MS system (Waters, Milford, MA) that included an Acquity UPLC system coupled to a Waters Q-ToF Premier high-resolution mass spectrometer. The ⁶⁸Ge/⁶⁸Ga generator was purchased from Ithemba Labs (South Africa) and ¹⁸F-fluoride was obtained from the NIH cyclotron facility.

Preparation of NOTA-PRGD2

NOTA-PRGD2 was synthesized following our previously reported procedure with modifications.¹⁵ Briefly, 7.0 mg (15.5 μmol) of *p*-SCN-Bn-NOTA in 50 μL of dimethyl sulfoxide (DMSO) was added to a 4 mL glass vial containing 21.0 mg (14 μmol) of PRGD2 and 20 μL of diisopropylethylamine in 0.3 mL N,N-dimethylformamide (DMF). After 1 h, the reaction was quenched with 20 μL of acetic acid in 1 mL water. The reaction mixture was purified with a preparative HPLC running a linear gradient starting from 6% A (0.1% TFA in acetonitrile) and 94% B (0.1% TFA in water) for 5 min and increasing to 65% A at 35 min with a flow rate of 12 mL/min. The fractions containing the desired product (55%) were collected and lyophilized to give 15.0 mg of white powder. The purity of the product was > 95% by analytical HPLC (*t_R* = 16.4 min). LC-MS: [MH]⁺=1989.69 (m/z), calc: 1988.91 (C₈₇H₁₂₈N₂₄O₂₈S).

Preparation of Al-NOTA-PRGD2

To a 1 mL V-vial containing 1.1 mg of NOTA-PRGD2 in 0.2 mL of deionized water was added 0.21 mg of aluminum chloride in 20 μL 0.5 M pH 4.0 sodium acetate buffer. The vial was sealed and the mixture was heated at 105 °C for 10 min and then injected onto a preparative RP HPLC C₁₈ column with a linear gradient starting from 6% A (0.1% TFA in acetonitrile) and 94% B (0.1% in water) for 5 min and increasing to 65% A at 35 min at the flow rate of 12 mL/min. A single peak at the retention time of 19.7 min was collected and analyzed with LC-MS. The peak had the [MH]⁺=2013.6660 (m/z) which matched the calculated mass for Al-NOTA-PRGD2 (C₈₇H₁₂₅AlN₂₄O₂₈S: 2012.8631). The sample was lyophilized overnight to give 1.1 mg of white powder (99%). The purity of the product was > 97% by analytical HPLC (Dionex, 4.6 × 150 mm) with a retention time of 15.5 min with a base line separation from the NOTA-PRGD2 (16.4 min).

Preparation of FAI-NOTA-PRGD2

To a 1 mL V-vial containing 0.2 mL of deionized water were added 10 μL of 2 mM aluminum chloride in 0.1 M pH 4.0 sodium acetate buffer and 7 μL of 3.0 mM sodium fluoride in 0.1 M pH 4.0 sodium acetate buffer. The mixture was heated at 100 °C for 10 min, and 5 μL of 2.5 mM NOTA-PRGD2 in 0.1 M pH 4.0 sodium acetate buffer was added to the reaction mixture, which was then heated at 100 °C for another 10 min. The solution was cooled and injected onto an analytical RP C₁₈ column (Vydac C₁₈) running a linear gradient starting from 5% A (0.1% TFA in acetonitrile) and 95% B (0.1% TFA in water) for 2 min and increasing to 65% A at 32 min at 1 mL/min. The peaks at 15.5 min and 15.7 were collected as a single fraction. The LC-MS analysis showed two mass components in this fraction with [MH]⁺=2013.67 (m/z) corresponding to the mass of Al-NOTA-PRGD2 (*R_t* = 15.5 min) and [MH]⁺=2033.65 (m/z) corresponding to FAI-NOTA-PRGD2 (calculated for C₈₇H₁₂₆AlFN₂₄O₂₈S: 2032.87).

Preparation of Ga-NOTA-PRGD2

To a 1 mL V-vial containing 2.6 mg of NOTA-PRGD2 in 0.3 mL of deionized water was add 0.5 mg of gallium chloride in 0.1 mL of 0.1 M pH 4.0 sodium acetate buffer. The mixture was heated at 80 °C for 10 min and then injected onto a preparative RP HPLC C₁₈ column running the same gradient as described above. A single peak at the retention time of 19.5 min was collected and lyophilized overnight to give 2.6 mg of white powder (99%). LC-MS: [MH]⁺=2056.0730 (m/z) corresponding to Ga-NOTA-PRGD2 (calculated for C₈₇H₁₂₅GaN₂₄O₂₈S: 2054.8072).

Preparation of 4-nitrophenyl 2-[¹⁸F]fluoropropionate

The 4-nitrophenyl [¹⁸F]-2-fluoropropionate was prepared on a GE TRACERLab FXN according to a published procedure¹⁹ with some modifications. For a typical run, [¹⁸F]fluoride was trapped on an ¹⁸F Separation Cartridge (CHROMAFIX, 30-PS-HCO₃) from a source vial containing the aqueous [¹⁸F]fluoride (3.7 GBq, 0.2 mL) by pulling the vacuum line. The activity was eluted to a glassy-carbon reaction vessel with 1 mL 90% acetonitrile containing 15.0 mg of K222 and 3.5 mg of potassium carbonate. The liquid in the reaction vessel was removed with vacuum to produce anhydrous [¹⁸F]fluoride. After cooling, 5 mg of ethyl 2-bromopropionate in 0.5 mL of acetonitrile was added to the reaction vessel and heated at 100 °C for 10 min to form ethyl 2-[¹⁸F]fluoropropionate. At the end the of the reaction, 125 μL of 0.2 N potassium hydroxide in 375 μL of acetonitrile was added to the reaction vessel, which was then heated at 100 °C for another 10 min to produce the potassium salt of 2-[¹⁸F]fluoropropionic acid. The solution was diluted with 1 mL of acetonitrile and the liquid was removed with vacuum, 20 mg of bis-4-nitrophenyl carbonate in 1 mL of acetonitrile was added to react with potassium 2-[¹⁸F]fluoropropionate to form 4-nitrophenyl 2-[¹⁸F]fluoropropionate at 100 °C for 10 min. After cooling, the reaction mixture was diluted with 1 mL of 25% acetonitrile/water with 5% acetic acid and loaded onto a semi-prep Phenomenex Luna C₁₈ column running at 5 mL/min with 40% acetonitrile/water containing 0.1% TFA as the mobile phase. The product was collected at the retention time of 21 min into a flask containing 30 mL of water with 0.1% acetic acid. The solution containing the desired product was passed through a Waters Sep-Pak Plus C₁₈ cartridge and the activity trapped on the cartridge was washed with 1 mL of water.

Preparation of [¹⁸F]FPPRGD2

The activity trapped on the C₁₈ cartridge as described above was eluted manually with 1 mL of methylene chloride into a 1 mL polypropylene tube and the water layer on top of the methylene chloride was removed by using a syringe. The methylene chloride in the tube was evaporated under argon flow at room temperature, and 1 mg of PRGD2 in 0.1 mL of DMSO containing 20 μL of diisopropylethylamine was added to the tube and heated at 80 °C for 10 min. At the end of the reaction, the reaction mixture was cooled and diluted with 0.7 mL of water containing 25 μL of acetic acid and loaded onto a semi-prep HPLC column (Vydac C₁₈) running a linear gradient starting from 5% A (0.1% TFA in acetonitrile) and 95% B (0.1% TFA in water) for 2 min and increasing to 65% A at 32 min at 5 mL/min. The desired product was collected at a retention time of 14 min and diluted with 10 mL water and trapped on a Varian Bond Elut C₁₈ column (100 mg). The radioactivity trapped on the C₁₈ column was eluted with 0.3 mL of 1 mM HCl-ethanol solution, and the ethanol was removed with argon flow, and the final product was then dissolved in PBS.

[¹⁸F]FAI-NOTA-PRGD2

Three μL of 2 mM aluminum chloride in 0.2 M pH 4 sodium acetate buffer was added to a 1 mL V-vial containing 0.1 mL of aqueous [¹⁸F]fluoride (0.37 GBq), which was then heated at 100 °C for 10 min to form the aluminum-fluoride complex. The vial was cooled, 6 μL of

2 mM NOTA-PRGD2 in 0.2 M pH 4 sodium acetate buffer was added, and then the vial was heated at 100 °C for another 10 min. At the end of the reaction, the mixture was injected onto an analytical HPLC column (Vydac C₁₈) running a linear gradient starting from 5% A (0.1% TFA in acetonitrile) and 95% B (0.1% TFA in water) for 2 min and increasing to 65% A at 32 min at 1 mL/min. The radioactive peak containing the desired product was collected at a retention time of 16 min and diluted with 15 mL of water and trapped on a Varian Bond Elut C₁₈ column (100 mg). The radioactivity trapped on the C₁₈ column was eluted with 0.3 mL of 80% ethanol/water with 2% acetic acid, the ethanol solution was evaporated with argon flow, and the final product was then dissolved in PBS. A separate procedure was performed without HPLC purification and the reaction mixture was directly loaded onto the C₁₈ cartridge.

[⁶⁸Ga]Ga-NOTA-PRGD2

The fresh ⁶⁸Ga activity was eluted from the ⁶⁸Ge/⁶⁸Ga generator with 0.6 M HCl at 0.5 mL per fraction into the 1.5 mL polypropylene tubes. The fraction containing the most radioactivity (~0.15 GBq) was added to 0.45 mL of 1M HEPES buffer and 15 µg of NOTA-PRGD2 in 5 µL of 0.2 M pH 4 sodium acetate buffer. The mixture was heated at 80 °C for 10 min. At the end of the reaction, the activity was loaded onto an analytical HPLC column (Vydac C₁₈) running a linear gradient starting from 5% A (0.1% TFA in acetonitrile) and 95% B (0.1% TFA in water) for 2 min and increasing to 65% A at 32 min at 1 mL/min. The desired product was collected at 16 min, diluted with 15 mL of water, and trapped onto a 100 mg Varian Bond Elut C₁₈ column. The radioactivity trapped on the C₁₈ column was eluted with 0.3 mL of 80% ethanol/water with 2% acetic acid, the ethanol solution was removed with argon flow, and the final product was re-dissolved in PBS. A separate procedure was performed without HPLC purification, and the reaction mixture was directly loaded onto the C₁₈ cartridge. The reactions were done at room temperature and at 80 °C. The crude mixture and purified product were also analyzed with analytical HPLC for their radiochemical purities.

Cell binding assay

The $\alpha_v\beta_3$ receptor binding assay was performed to determine binding affinities of E[c(RGDyK)]₂ analogs. Briefly, U87MG cell line was cultured in DMEM medium (GIBCO) containing 10% (v/v) fetal bovine serum (GIBCO) supplemented with penicillin (100 µg/ml), streptomycin (100 µg/ml), non-essential amino acids (100 µM) and sodium pyruvate (1 mM) at 37 °C with 5% CO₂. When grew up to 80% confluence, cells were scraped off and suspended with binding buffer [25 mM 2-amino-2-(hydroxymethyl)-1,3-propanediol, hydrochloride (Tris-HCl), pH 7.4, 150 mM NaCl, 1 mM CaCl₂, 0.5 mM MgCl₂ and 1 mM MnCl₂, 0.1% bovine serum albumin (BSA)] at a final concentration of 2×10⁶ cells/ml. In a 96-well plate, 1×10⁵ U87 MG cells/well were incubated with ¹²⁵I-Echistatin (0.74 kBq/well, PerkinElmer, Inc) in binding buffer in the presence of different concentrations of E[c(RGDyK)]₂ analogs at room temperature for 1h. After incubation, the plate was washed three times with phosphate buffered saline (PBS) containing 0.1% BSA, and the radioactivity was measured by γ -counting. The EC₅₀ values were calculated by nonlinear regression analysis using the GraphPad Prism computer-fitting program (GraphPad Software, Inc., San Diego, CA). Each data point is a result of the average of triplicate wells.

Preparation of animal tumor models

All animal studies were conducted in accordance with the principles and procedures outlined in the Guide for the Care and Use of Laboratory Animals and were approved by the Institutional Animal Care and Use Committee of the Clinical Center, NIH. The human glioblastoma cell line U87MG was grown in DMEM medium supplemented with 10% fetal

bovine serum (FBS), 100 IU/mL penicillin, and 100 µg/mL streptomycin (Invitrogen), and in a humidified atmosphere containing 5% CO₂ at 37°C. The cells were harvested by trypsinization with trypsin/EDTA. The U87MG tumor model was developed in 5 to 6 week old female athymic nude mice (Harlan Laboratories) by injection of 5×10⁶ cells in their right shoulders. Tumor growth was monitored using caliper measurements of perpendicular axes of the tumor. The mice underwent small-animal PET studies when the tumor volume reached 100–300 mm³ (3 – 4 weeks after inoculation).

MicroPET imaging and analysis

PET scans and image analysis were performed using an Inveon microPET scanner (Siemens Medical Solutions). About 3.7 MBq of ¹⁸F or ⁶⁸Ga labeled tracer was administered via tail vein injection under isoflurane anesthesia. For blocking study, about 300 µg of unlabeled dimeric RGD peptide E[c(RGDyK)]₂ was injected 30 min before the [¹⁸F]FAI-NOTA-PRGD2. Five-minute static PET images were acquired at 30 min, 1 h and 2 h postinjection (n = 3–5 per group). The images were reconstructed using a two-dimensional ordered-subset expectation maximum (2D OSEM) algorithm, and no correction was applied for attenuation or scatter. For each scan, regions of interest (ROIs) were drawn using vendor software (ASI Pro 5.2.4.0) on decay-corrected whole-body coronal images. The radioactivity concentrations (accumulation) within the tumors, muscle, liver, and kidneys were obtained from mean pixel values within the multiple ROI volume and then converted to MBq per milliliter. These values were then divided by the administered activity to obtain (assuming a tissue density of 1 g/ml) an image-ROI-derived percent injected dose per gram (%ID/g).

Biodistribution study of [¹⁸F]FAI-NOTA-PRGD2

Immediately after PET imaging, the tumor-bearing mice with or without blocking dose were sacrificed and dissected. Blood, tumor, major organs, and tissues were collected and wet-weighed. The radioactivity in the wet whole tissue was measured with a γ-counter (Perkin-Elmer). The results were expressed as percentage of injected dose per gram of tissue (%ID/g). Values were expressed as mean ± SD (n = 4 per group).

In vitro stability of [¹⁸F]FAI-NOTA-PRGD2

About 5.6 MBq of [¹⁸F]FAI-NOTA-PRGD2 in 50 µL of PBS was added to 400 µL of mouse serum and incubated at 37 °C. About 60 µL of this serum sample was taken out at 1, 30, 60 and 120 min and put into a plastic tube. An equal volume of acetonitrile was added to each tube and centrifuged at 6000 rpm for 8 min. The supernatant was separated from the pellet and both the supernatant and pellet were measured for their radioactivity. The supernatant was diluted with 300 µL of PBS and injected on to an analytical HPLC. The tube was measured for its radioactivity before and after HPLC injection. The radioactivity coming out of HPLC column was also collected and measured.

Results

Chemistry

The structures of PEGylated dimeric RGD peptides are shown in Figure 1. The 2-fluoropropanoyl labeled PRGD2 is designated as FPPRGD2. S-2-(4-Isothiocyanatobenzyl)-1,4,7-triazacyclononane-1,4,7-triacetic Acid is designated as p-SCN-Bn-NOTA. The p-SCN-Bn-NOTA labeled PRGD2 is designated as NOTA-PRGD2. The aluminum NOTA-PRGD2 complex is designated as Al-NOTA-PRGD2, and the aluminum fluoride complex of NOTA-PRGD2 is designated as FAI-NOTA-PRGD2. Gallium NOTA-PRGD2 complex is designated as Ga-NOTA-PRGD2.

NOTA-PRGD2, AI-NOTA-PRGD2, and Ga-NOTA-PRGD2 were prepared at mg scale that can be lyophilized and weighed for further use. The yield of AI-NOTA-PRGD2 and Ga-NOTA-PRGD2 was almost quantitative. Chemical purities of these compounds were > 97% determined by analytical HPLC analysis. FAI-NOTA-PRGD2 was prepared in small-scale reaction, collected from HPLC and used directly as the reference compound. The identities of non-radioactive compounds were determined by LC-MS, which observed m/z ions that matched their calculated molecular weights. Preparation of FAI-NOTA-PRGD2 yielded a mixture of FAI-NOTA-PRGD2 and AI-NOTA-PRGD2 that were not separable by HPLC.

In order to confirm that adding metal NOTA complex to the PRGD2 do not affect the binding affinity of the peptides to integrin receptors, we performed competitive cell binding assays with ^{125}I -echistatin as the radioligand in integrin $\alpha_v\beta_3$ positive U87MG cells. Results of the cell-binding assays were plotted and fitted to sigmoid curves for the displacement of ^{125}I -echistatin from U87MG cells (Figure 2A). The IC_{50} values are listed in Figure 2B. The results indicated that the adding metal NOTA complex to PRGD2 had up to 2-fold increase on the binding affinity of the peptides compared to that of FPPRGD2.

Radiochemistry

The radiolabeling of the three compounds is summarized in Table 1. The radiochemical yield for 4-nitrophenyl 2- ^{18}F fluoropropionate prepared from Tracer FX-FN system was around 20–25%, and the yield for coupling of 4-nitrophenyl 2- ^{18}F fluoropropionate with PRGD2 was over 75%. The overall yield was 10–15% (uncorrected) with a total synthesis time of around 3 h and the measured specific activity was 114 ± 72 GBq/ μmol (EOB). The labeling efficiency for ^{18}F FAL-NOTA-PRGD2 varied between 5 and 25%, depending on the reaction volumes. When the reaction volume was between 50 and 100 μL , the yield was consistently between 20–25% (uncorrected). The total synthesis time was about 40 min with HPLC purification and about 25 min without HPLC purification. The radiochemical purity was over 97%. The radiochemical yield for ^{68}Ga Ga-NOTA-PRGD was about 70% (uncorrected) with HPLC in a total synthesis time of 30 min.

Purification of radiolabeled products by solid phase extraction

To further simplify the labeling procedure, the solid phase extraction method was used to prepare both ^{18}F FAI-NOTA-PRGD2 and ^{68}Ga Ga-NOTA-PRGD2. The tracer could be prepared in about 15 min. Without the HPLC purification the specific activity was determined by the amount of peptide used, assuming the complete recovery of peptide and the amount of radioactivity used. In our preparation of these two tracers, 12 nmol of PRGD2 was used to make ^{18}F FAI-NOTA-PRGD2, and 8 nmol of peptide was used to make ^{68}Ga Ga-NOTA-PRGD2. In this study, ^{18}F activity was limited to 0.37–1.5 GBq, and ^{68}Ga activity limited to 0.15–0.20 GBq. For a 37 MBq of product, at the end of synthesis the specific activity was 6.14 GBq/ μmol for ^{18}F FAI-NOTA-PRGD2 and 9.25 GBq/ μmol for ^{68}Ga Ga-NOTA-PRGD2. For a 0.37 GBq of product the specific activities were 30.71 GBq/ μmol and 46.25 GBq/ μmol respectively for ^{18}F FAI-NOTA-PRGD2 and ^{68}Ga Ga-NOTA-PRGD2. For ^{68}Ga Ga-NOTA-PRGD2, when only solid phase extraction was used the radiochemical yield was 40% at room temperature and reached over 90% at 80 $^{\circ}\text{C}$. The radiochemical purity was also > 97% for room temperature reaction with a slight decrease of radiochemical purity (95%) at 80 $^{\circ}\text{C}$.

In vitro stability of the radiotracers

Both ^{68}Ga Ga-NOTA-PRGD2 and ^{18}F FAI-NOTA-PRGD2 were stable in PBS at room temperature. After 4 hours, the radiochemical purities were > 95% with HPLC analysis. We also tested the stability of ^{18}F FAI-NOTA-PRGD2 in mouse serum up to 2 hours at 37 $^{\circ}\text{C}$. After treating the serum samples with acetonitrile and centrifugation, 85% of radioactivity

was in solution. The recovery of radioactivity from HPLC was >96% without any detectable F-18 fluoride. The parent compound at 1, 30, 60, and 120 min constituted 96.8 %, 96.6 %, 95.1 % and 95.0 % of recovered radioactivity, respectively.

MicroPET imaging

After radiolabeling, we applied the three imaging probes to *in vivo* PET imaging with U87MG tumor bearing mice. The representative decay-corrected coronal images at different time points after injection of the radiotracers are shown in Figures 3–5. The U87MG tumors were clearly visualized with good tumor-to-background contrast with all of the tracers as early as 30 min post-injection (p.i.). The quantitative tracer uptake of tumors and major organs is summarized in Table 2, expressed as % ID/g. At 60 min p.i., the tumor uptake of [¹⁸F]FPPRGD2 was 2.56 ± 0.48 % ID/g (n = 5), which was consistent with a previous report.¹⁸ As for [⁶⁸Ga]Ga-NOTA-PRGD, the tumor uptake was 2.98 ± 0.53 % ID/g (n = 3). The tumor uptake of [¹⁸F]FAI-NOTA-PRGD2 was 3.92 ± 0.18 % ID/g (n = 4), which was significantly higher than that of the other two tracers (p < 0.05). Besides tumor uptake, all tracers showed relatively high kidney accumulation, especially at the early time point (30 min p.i.), then dropped significantly afterwards, indicating rapid renal clearance. All three tracers showed relatively low liver uptake. Compared with the other two tracers, [¹⁸F]FPPRGD2 showed faster clearance from tumors. We believe this may be a consequence of the lower binding affinity of FPPRGD2 as determined by *in vitro* cell binding affinity study.

Biodistribution Studies

In order to further confirm the PET imaging quantification, the biodistribution of [¹⁸F]FAI-NOTA-PRGD2 with and without blocking dose was evaluated in U87MG tumor-bearing athymic nude mice immediately after PET imaging (Fig. 6). Consistent with PET imaging data, the tumor uptake measured by direct tissue sampling and gamma-counting was 1.45 ± 0.47 % ID/g at the 2 h time point. The tracer accumulations in the kidneys and liver were 4.88 ± 0.82 and 1.47 ± 0.50 % ID/g, respectively, at 2 h p.i. In the blocking experiment, U87MG tumor showed significantly decreased accumulation of [¹⁸F]FAI-NOTA-PRGD2 with an uptake value of 0.15 ± 0.04 % ID/g (p < 0.001).

Discussion

Labeling peptides and proteins with ¹⁸F is usually achieved using prosthetic groups. The required multi-step procedure for preparation of the prosthetic group, its purification, subsequent protein coupling step, and final purification results in relatively low overall radiochemical yield. In addition, multistep syntheses are more difficult to automate.²⁵ F-18 click chemistry has been used in several studies to label peptides.²⁶ However, it requires the preparation of azide or alkyne functional group modified peptides and two radiochemical synthesis steps, and in some cases it involves volatile [¹⁸F]-azide synthon. Alternatively, several groups including our lab have developed direct labeling methods of peptides with ¹⁸F.^{21, 27, 28}

We have applied [¹⁸F]FPPRDG2 to monitor the treatment effect of various anti-cancer drugs longitudinally on mouse tumor models.^{7–9} The routine preparation of [¹⁸F]FPPRDG2, which is a 3 h procedure, is quite challenging. Currently, there is no commercially available automated synthesizer that is capable of producing [¹⁸F]FPPRDG2 without major modifications. McBride and Laverman et al.^{23, 24, 29} reported the method of using the [¹⁸F]fluoride-aluminum-NOTA complex for labeling peptides. Although the radiolabeling conditions required heating, the inherent thermal stability of RGD peptides suggested that

they would be good substrates for this radiolabeling method. The precursor for making [^{18}F]FPPRDG2 was chosen as building block for direct comparison studies.

The dimeric PRGD2 peptide was selected for this comparison study for three major reasons. Dimeric PRGD2 showed higher affinity for $\alpha_v\beta_3$ integrin receptor than its monomeric counterpart. PEGylation improved the properties by reducing the renal retention of this class of compounds. Finally the terminal amine of the PEG moiety served as an attachment point of radiolabel.¹⁸ Attachment of a NOTA functional group to this terminal amine of PRGD2 provided a chelate that can be effectively utilized for both [^{18}F]fluoride-aluminum and ^{68}Ga . In this study, we successfully prepared [^{18}F]FAI-NOTA-PRGD2 and compared its imaging quality with that of [^{18}F]FPPRDG2 and [^{68}Ga]Ga-NOTA-PRGD2 as an integrin $\alpha_v\beta_3$ imaging agent in U87MG mouse tumor model. The results were very encouraging and further studies are needed to determine if [^{18}F]FAI-NOTA-PRGD2 is suitable for clinical use.

We applied HPLC columns to purify labeled NOTA complexes. The [^{18}F]FAI-NOTA-PRGD2 was eluted as a single radioactive peak. It overlapped with Al-NOTA-PRGD2 complex and had a base line separation from NOTA-PRGD2. It has been reported that when NOTA was used as the chelator, two inter-changeable radioactive peaks were formed.²⁹ This was explained as the formation of two isomers of the complex. However, in our preparation only a single radioactive peak was observed. Since [^{18}F]FAI-NOTA-PRGD2 was not separated from Al-NOTA-PRGD2 in our case, the specific activity was determined by the amount of aluminum chloride used. Our labeling yield was lower than reported by Laverman et al.,²⁹ but the amount of peptide used in our reaction was also less. In order to allow radiolabeling without HPLC purification, we limited the use of peptide to a 2 to 1 ratio with aluminum chloride. Although others have used a QMA column to purify and concentrate ^{18}F -fluoride,²³ in our hands aqueous ^{18}F activity was used directly from the target, and the QMA treatment did not change the labeling yield. Generator produced ^{68}Ga with its 68 min half-life is an attractive alternative for institutions without a cyclotron. In this study, the same peptide was used for labeling Ga-68 for a direct comparison. Labeling yield for forming Ga-68 complex was higher than for forming F-18 FAI complex, and the amount of peptide needed was also less.

When the solid phase extraction was used for the preparation of both [^{18}F]FAI-NOTA-PRGD2 and [^{68}Ga]Ga-NOTA-PRGD2, the tracer could be prepared in about 15 to 25 min. Compared with that of [^{18}F]FPPRDG2, this procedure is tremendously time saving. Moreover, with a scale-up preparation for a 0.37 GBq of product, the specific activity went up to 30.7 GBq/ μmol and 46.2 GBq/ μmol respectively for [^{18}F]FAI-NOTA-PRGD2 and [^{68}Ga]Ga-NOTA-PRGD2. These specific activity levels should meet the requirement for clinical studies. For Ga-68 labeling, specific activity can be further increased by using less peptide. Another important aspect of using solid phase extraction is that the standard kit can be formulated and distributed. This is especially important for multiple-center studies, since the amount of peptide used can be predetermined precisely.

After applying the tracers to *in vivo* PET imaging, we found that FPPRDG2 showed tumor uptake and major organ distribution that were similar to those in one of our previous studies.¹⁸ However, the tumor uptake of [^{68}Ga]Ga-NOTA-PRGD2 was somewhat lower than that in another study.²² The reason for this is unclear, and we will investigate the *in vivo* behavior of this tracer further for potential clinical translation. Another issue is that both [^{18}F]FAI-NOTA-PRGD2 and [^{68}Ga]Ga-NOTA-PRGD2 showed longer tumor retention than that of [^{18}F]FPPRDG2 in U87MG tumors. Although we do not have a definitive explanation for this, we cannot exclude the possibility of transchelation of the metal ions within the tumor region.

Conclusion

Both [^{18}F]FAI-NOTA-PRGD2 and [^{68}Ga]Ga-NOTA-PRGD2 can be prepared with or without HPLC purification in a much simpler fashion than [^{18}F]FPPRGD2. Moreover, these two new radiotracers have imaging properties and pharmacokinetics that are comparable, or superior to, those of [^{18}F]FPPRGD2. Considering the ease of preparation and imaging quality, [^{18}F]FAI-NOTA-PRGD2 and [^{68}Ga]Ga-NOTA-PRGD2 are promising alternatives to [^{18}F]FPPRGD2 for PET imaging of tumor $\alpha_v\beta_3$.

Acknowledgments

This project was supported by the Intramural Research Program of the National Institute of Biomedical Imaging and Bioengineering (NIBIB), National Institutes of Health (NIH) and the International Cooperative Program of the National Science Foundation of China (NSFC) (81028009). We thank Dr. Henry S. Eden for proof-reading the manuscript.

References

1. Folkman J. Tumor angiogenesis: therapeutic implications. *N Engl J Med.* 1971; 285:1182–6. [PubMed: 4938153]
2. Stupack DG, Cheresh DA. Integrins and angiogenesis. *Curr Top Dev Biol.* 2004; 64:207–38. [PubMed: 15563949]
3. Niu G, Chen X. Why integrin as a primary target for imaging and therapy. *Theranostics.* 2011; 1:30–47. [PubMed: 21544229]
4. Beer AJ, Kessler H, Wester HJ, Schwaiger M. PET imaging of integrin $\alpha_v\beta_3$ expression. *Theranostics.* 2011; 1:48–57. [PubMed: 21547152]
5. Zhou Y, Chakraborty S, Liu S. Radiolabeled cyclic RGD peptides as radiotracers for imaging tumors and thrombosis by SPECT. *Theranostics.* 2011; 1:58–82. [PubMed: 21547153]
6. Morrison M, Cuthbertson A. Integrin imaging to evaluate treatment response. *Theranostics.* 2011; 1:149–153. [PubMed: 21547157]
7. Sun X, Yan Y, Liu S, Cao Q, Yang M, Neamati N, Shen B, Niu G, Chen X. ^{18}F -FPPRGD2 and ^{18}F -FDG PET of response to Abraxane therapy. *J Nucl Med.* 2011; 52:140–6. [PubMed: 21149494]
8. Yang M, Gao H, Sun X, Yan Y, Quan Q, Zhang W, KAM, Rosenblum MG, Niu G, Chen X. Multiplexed PET probes for imaging breast cancer early response to VEGF $_{121}$ /rGel treatment. *Mol Pharm.* 2011; 8:621–628. [PubMed: 21280671]
9. Yang M, Gao H, Yan Y, Sun X, Chen K, Quan Q, Lang L, Kiesewetter D, Niu G, Chen X. PET imaging of early response to the tyrosine kinase inhibitor ZD4190. *Eur J Nucl Med Mol Imaging.* 2011; 38:1237–1247. [PubMed: 21360246]
10. Noiri E, Goligorsky MS, Wang GJ, Wang J, Cabahug CJ, Sharma S, Rhodes BA, Som P. Biodistribution and clearance of $^{99\text{m}}\text{Tc}$ -labeled Arg-Gly-Asp (RGD) peptide in rats with ischemic acute renal failure. *J Am Soc Nephrol.* 1996; 7:2682–8. [PubMed: 8989749]
11. Ahmadi M, Sancey L, Briat A, Riou L, Boturyn D, Dumy P, Fagret D, Ghezzi C, Vuillez JP. Chemical and biological evaluations of an ^{111}In -labeled RGD-peptide targeting integrin $\alpha_v\beta_3$ in a preclinical tumor model. *Cancer Biother Radiopharm.* 2008; 23:691–700. [PubMed: 19111043]
12. Chen X, Park R, Shahinian AH, Tohme M, Khankaldyyan V, Bozorgzadeh MH, Bading JR, Moats R, Laug WE, Conti PS. ^{18}F -labeled RGD peptide: initial evaluation for imaging brain tumor angiogenesis. *Nucl Med Biol.* 2004; 31:179–89. [PubMed: 15013483]
13. Chen X, Liu S, Hou Y, Tohme M, Park R, Bading JR, Conti PS. MicroPET imaging of breast cancer α_v -integrin expression with ^{64}Cu -labeled dimeric RGD peptides. *Mol Imaging Biol.* 2004; 6:350–9. [PubMed: 15380745]
14. Jeong JM, Hong MK, Chang YS, Lee YS, Kim YJ, Cheon GJ, Lee DS, Chung JK, Lee MC. Preparation of a promising angiogenesis PET imaging agent: ^{68}Ga -labeled c(RGDyK)-isothiocyanatobenzyl-1,4,7-triazacyclononane-1,4,7-triacetic acid and feasibility studies in mice. *J Nucl Med.* 2008; 49:830–6. [PubMed: 18413379]

15. Li ZB, Chen K, Chen X. ^{68}Ga -labeled multimeric RGD peptides for microPET imaging of integrin $\alpha\text{v}\beta 3$ expression. *Eur J Nucl Med Mol Imaging*. 2008; 35:1100–8. [PubMed: 18204838]
16. Jacobson O, Zhu L, Niu G, Weiss ID, Szajek LP, Ma Y, Sun X, Yan Y, Kiesewetter DO, Liu S, Chen X. MicroPET imaging of integrin $\alpha\text{v}\beta 3$ expressing tumors using ^{89}Zr -RGD Peptides. *Mol Imaging Biol*. 2010 Dec 16. [Epub ahead of print].
17. Dijkgraaf I, Liu S, Kruijtzter JA, Soede AC, Oyen WJ, Liskamp RM, Corstens FH, Boerman OC. Effects of linker variation on the in vitro and in vivo characteristics of an ^{111}In -labeled RGD peptide. *Nucl Med Biol*. 2007; 34:29–35. [PubMed: 17210459]
18. Liu S, Liu Z, Chen K, Yan Y, Watzlowik P, Wester HJ, Chin FT, Chen X. ^{18}F -labeled galacto and PEGylated RGD dimers for PET imaging of $\alpha\text{v}\beta 3$ integrin expression. *Mol Imaging Biol*. 2010; 12:530–8. [PubMed: 19949981]
19. Chin FT, Shen B, Liu S, Berganos RA, Chang E, Mittra E, Chen X, Gambhir SS. First Experience with clinical-grade [^{18}F]FPPRGD2: An automated multi-step radiosynthesis for clinical PET studies. *Mol Imaging Biol*. 2011 Mar 12. [Epub ahead of print].
20. Zhang X, Xiong Z, Wu Y, Cai W, Tseng JR, Gambhir SS, Chen X. Quantitative PET imaging of tumor integrin $\alpha\text{v}\beta 3$ expression with ^{18}F -FRGD2. *J Nucl Med*. 2006; 47:113–21. [PubMed: 16391195]
21. Jacobson O, Zhu L, Ma Y, Weiss ID, Sun X, Niu G, Kiesewetter DO, Chen X. Rapid and simple one-step F-18 labeling of peptides. *Bioconjug Chem*. 2011; 22:422–8. [PubMed: 21338096]
22. Liu Z, Niu G, Shi J, Liu S, Wang F, Chen X. ^{68}Ga -labeled cyclic RGD dimers with Gly3 and PEG4 linkers: promising agents for tumor integrin $\alpha\text{v}\beta 3$ PET imaging. *Eur J Nucl Med Mol Imaging*. 2009; 36:947–57. [PubMed: 19159928]
23. McBride WJ, D'Souza CA, Sharkey RM, Karacay H, Rossi EA, Chang CH, Goldenberg DM. Improved ^{18}F labeling of peptides with a fluoride-aluminum-chelate complex. *Bioconjug Chem*. 2010; 21:1331–40. [PubMed: 20540570]
24. McBride WJ, Sharkey RM, Karacay H, D'Souza CA, Rossi EA, Laverman P, Chang CH, Boerman OC, Goldenberg DM. A novel method of ^{18}F radiolabeling for PET. *J Nucl Med*. 2009; 50:991–8. [PubMed: 19443594]
25. Jacobson O, Chen X. PET designated fluoride-18 production and chemistry. *Curr Top Med Chem*. 2010; 10:1048–59. [PubMed: 20388116]
26. Thonon D, Kech C, Paris J, Lemaire C, Luxen A. New strategy for the preparation of clickable peptides and labeling with 1-(azidomethyl)-4- ^{18}F -fluorobenzene for PET. *Bioconjug Chem*. 2009; 20:817–23. [PubMed: 19323495]
27. Hohne A, Mu L, Honer M, Schubiger PA, Ametamey SM, Graham K, Stellfeld T, Borkowski S, Berndorff D, Klar U, Voigtman U, Cyr JE, Friebe M, Dinkelborg L, Srinivasan A. Synthesis, ^{18}F -labeling, and in vitro and in vivo studies of bombesin peptides modified with silicon-based building blocks. *Bioconjug Chem*. 2008; 19:1871–9. [PubMed: 18754574]
28. Mu L, Hohne A, Schubiger PA, Ametamey SM, Graham K, Cyr JE, Dinkelborg L, Stellfeld T, Srinivasan A, Voigtman U, Klar U. Silicon-based building blocks for one-step ^{18}F -radiolabeling of peptides for PET imaging. *Angew Chem Int Ed Engl*. 2008; 47:4922–5. [PubMed: 18496798]
29. Laverman P, McBride WJ, Sharkey RM, Eek A, Joosten L, Oyen WJ, Goldenberg DM, Boerman OC. A novel facile method of labeling octreotide with ^{18}F -fluorine. *J Nucl Med*. 2010; 51:454–61. [PubMed: 20150268]

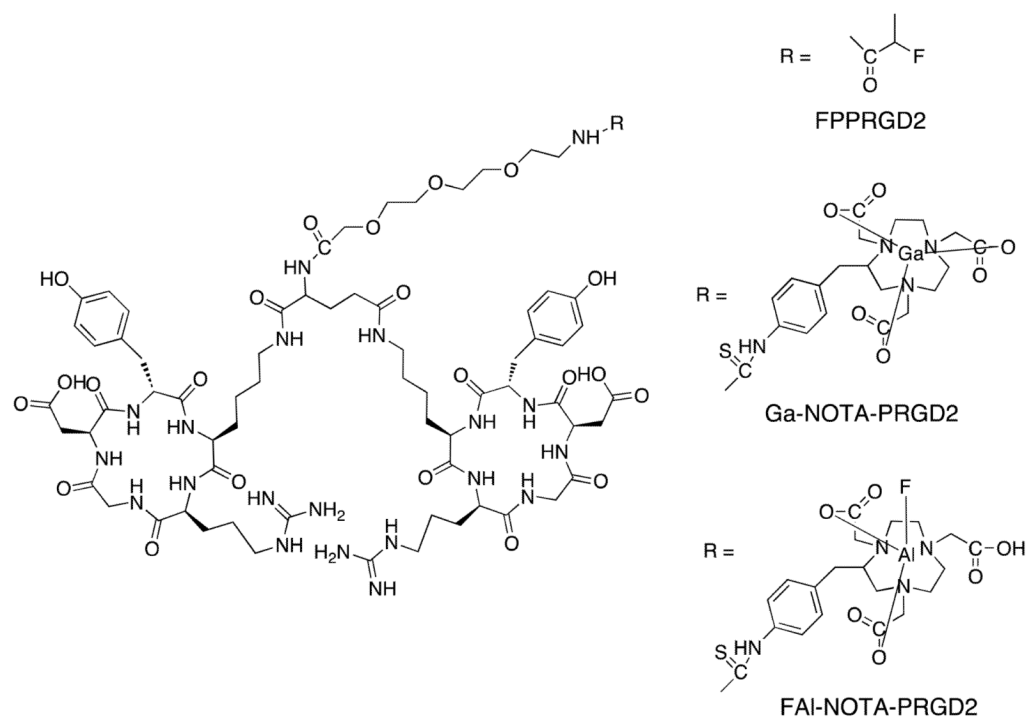


Figure 1.
Chemical structures of dimeric RGD peptides.

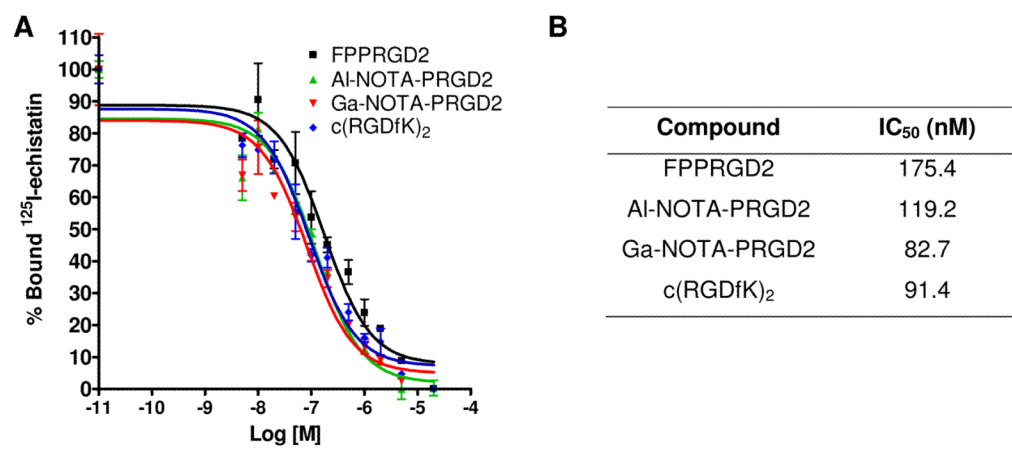


Figure 2. (A) Cell binding assay of RGD peptides in U87MG cells; (B) IC₅₀ of each RGD compound (n = 3).

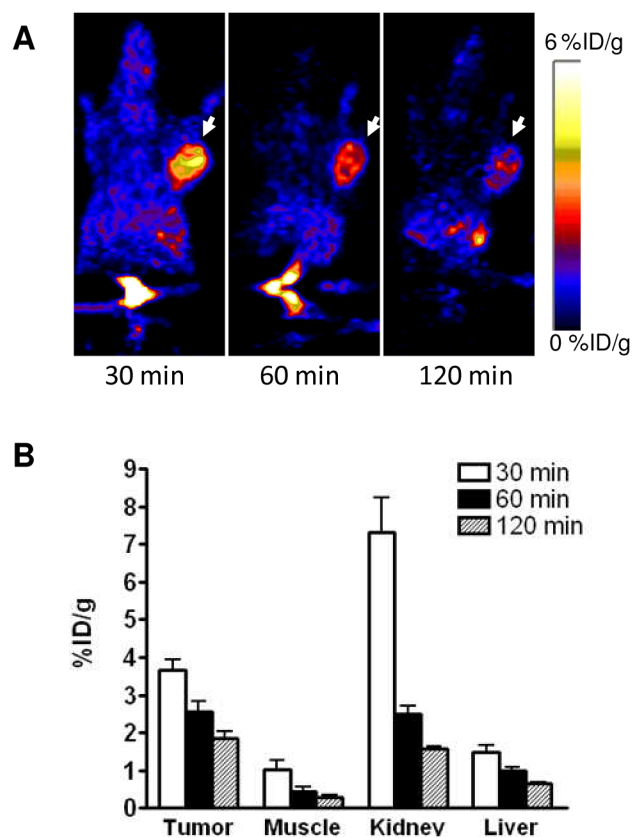


Figure 3. *In vivo* PET imaging of U87MG xenografted mice by [^{18}F]FPPRGD2. (A) Decay-corrected whole-body coronal microPET images of U87MG tumor-bearing mice at 30, 60, and 120 min after injection of 3.7 MBq of [^{18}F]FPPRGD2. Tumors are indicated by arrows. (B) Quantification of [^{18}F]FPPRGD2 in U87MG tumor, liver, kidneys and muscle. ROIs are shown as mean %ID/g \pm SD.

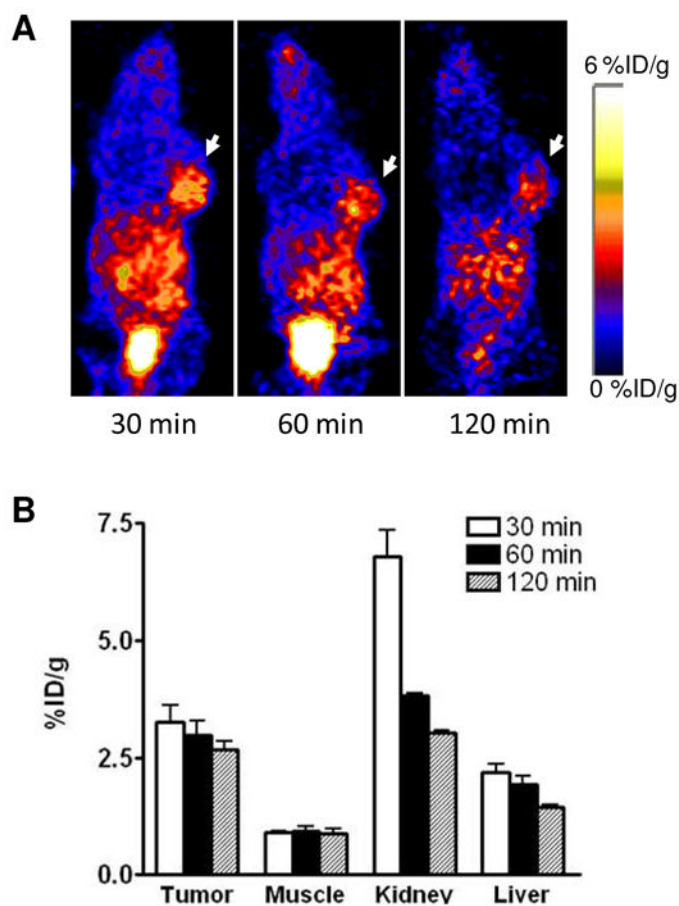


Figure 4. *In vivo* PET imaging of U87MG xenografted mice by [^{68}Ga]Ga-NOTA-PRGD2. (A) Decay-corrected whole-body coronal microPET images of U87MG tumor-bearing mice at 30, 60, and 120 min after injection of 3.7 MBq of [^{68}Ga]Ga-NOTA-PRGD2. Tumors are indicated by arrows. (B) Quantification of [^{68}Ga]Ga-NOTA-PRGD2 in U87MG tumor, liver, kidneys and muscle. ROIs are shown as mean %ID/g \pm SD.

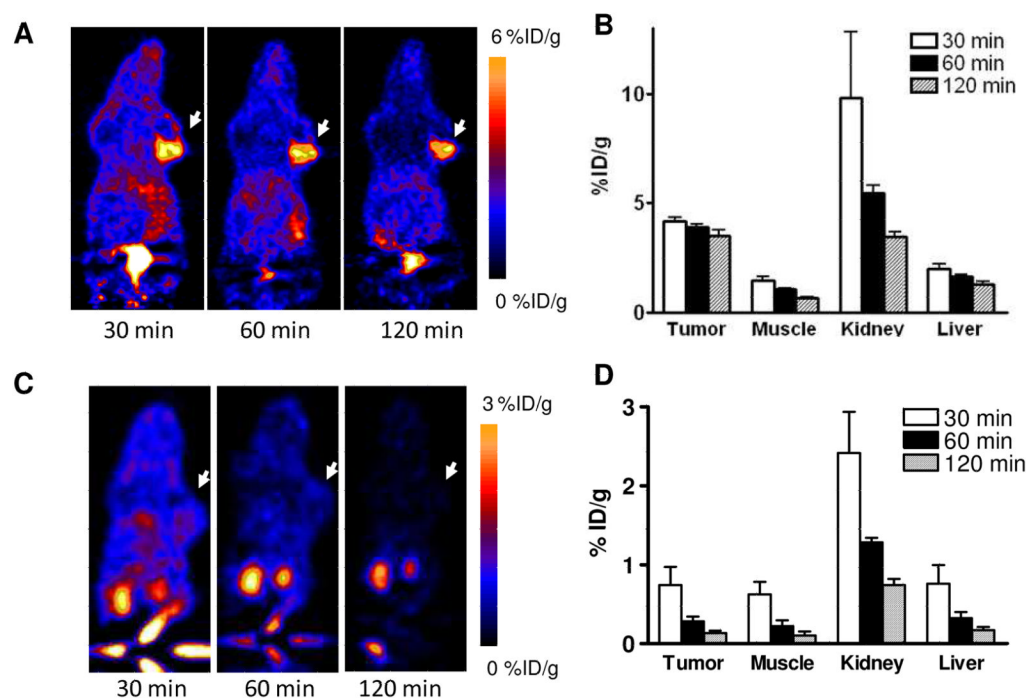


Figure 5.

In vivo PET imaging of U87MG xenografted mice with [^{18}F]FAI-NOTA-PRGD2. Decay-corrected whole-body coronal microPET images of U87MG tumor-bearing mice at 30, 60, and 120 min after injection of 3.7 MBq of [^{18}F]FAI-NOTA-PRGD2 without (A) and with (C) blocking dose. Tumors are indicated by arrows. Quantification of [^{18}F]FAI-NOTA-PRGD2 in U87MG tumor, liver, kidneys and muscle without (B) and with (D) blocking dose. ROIs are shown as mean %ID/g \pm SD.

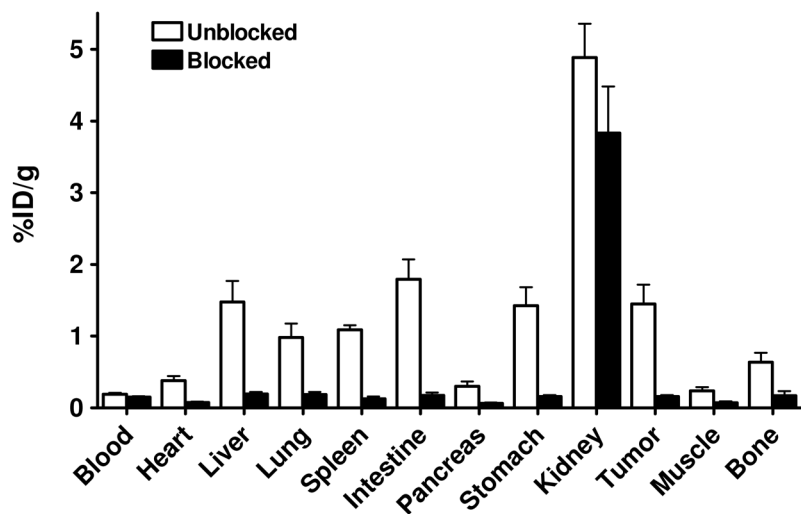


Figure 6. *Ex vivo* biodistribution of [^{18}F]FAI-NOTA-PRGD2 (3.7 MBq per mouse) in U87MG tumor bearing nude mice at 2 h time points after microPET scans with or without unlabeled RGD peptide as blocking agent. Columns, mean %ID/g (n = 4 per group); bars, SD.

Table 1

Comparison of reaction condition and yield of [¹⁸F]FAI-NOTA-PRGD2, [¹⁸F]FPPRDG2 and [⁶⁸Ga]Ga-NOTA-PRGD2

Tracer Name	Total Time (min)	HPLC	Reaction Temperature	Labeling yield (n = 5)
[¹⁸ F]FPPRDG2	180	YES	80°C	10–15%
[⁶⁸ Ga]NOTA-PRGD2	30	YES	80°C	75%
	15	NO	RT	40%
[¹⁸ F]FAI-NOTA-PRGD2	40	YES	100°C	5–25%
	25	NO	100°C	5–25%

Table 2

Biodistribution of dimeric RGD peptide tracers in U87MG tumor-bearing mice, determined by PET imaging (% ID/g \pm SD)

	$[^{18}\text{F}]\text{FPPRDG2}$			$[^{68}\text{Ga}]\text{NOTA-PRGD2}$			$[^{18}\text{F}]\text{FAI-NOTA-PRGD2}$		
	30 min	60 min	120 min	30 min	60 min	120 min	30 min	60 min	120 min
Tumor:	3.65 \pm 0.51	2.56 \pm 0.48	1.85 \pm 0.30	3.25 \pm 0.62	2.98 \pm 0.53	2.66 \pm 0.32	4.20 \pm 0.23	3.92 \pm 0.18	3.53 \pm 0.45
Muscle:	1.03 \pm 0.42	0.44 \pm 0.22	0.28 \pm 0.09	0.91 \pm 0.02	0.92 \pm 0.18	0.87 \pm 0.18	1.49 \pm 0.25	1.07 \pm 0.06	0.68 \pm 0.06
Kidney:	7.31 \pm 1.61	2.49 \pm 0.36	1.57 \pm 0.09	6.80 \pm 0.97	3.81 \pm 0.08	3.02 \pm 0.11	9.80 \pm 5.21	5.45 \pm 0.61	3.46 \pm 0.44
Liver:	1.48 \pm 0.33	1.00 \pm 0.11	0.64 \pm 0.05	2.18 \pm 0.30	1.92 \pm 0.34	1.44 \pm 0.08	2.02 \pm 0.32	1.66 \pm 0.13	1.28 \pm 0.28